Chiang Mai J. Sci. 2011; 38(2) : 166-175
www.science.cmu.ac.th/journal-science/josci.html
Contributed Paper

Ear Based Personal Identification Approach Forensic Science Tasks

Rerkchai Fooprateepsiri* and Werasak Kurutach**
Faculty of Information Science and Technology, Mahanakorn University and Technology,
140 Cheum-sampan rd., Nongchok, Bangkok, 10530, Thailand.
Author for correspondence; e-mail: * rerkchai@mut.ac.th, ** werasak@mut.ac.th

Received: 22 September 2010
Accepted: 17 January 2011

Abstract

Ear has been suggested by the researchers that the shape and features of ear are unique for each person and invariant with age. This paper proposes a robust method for ear based personal identification under environment of variant scaling, rotation and image reflection. Techniques introduced in this work are composed of two parts. The first one is the detection of ear features by using the concepts of multi-resolution Trace transform and Fourier transform. Then, in the second part, modified Hausdorff distance is employed to measure and determine of similarity between the models and tested images. Finally, our method is evaluated with experiments on images from the CMU PIE database. The extensive experimental results show that the average of accuracy rate of ear recognition with variant scaling, rotation and image reflection is higher than 97 %.

Keywords: biometric, forensic Science, trace transform, hausdorff distance.

1. Introduction

Ear features have been used for many years in task of forensic science for personal identification. This is because ear is a stable biometric and invariant with age change. Moreover, it has all the properties trait should have, i.e. uniqueness, universality, permanence and collectability. Ear does not have a completely random structure. As shows in [Figure 1], the standard features of the ear. Unlike face structure, ear has no expression changes, makeup effects and the color is constant trough out the ear. Ear was first used for identification of human being by Iannarelli [1] who used manual techniques to identify ear images. Samples of over 10,000 ears were studied to prove the distinctiveness of ears. Structure of ear does not change radically over time. The medical literature [2] provides information that ear growth is proportional after first four months of birth and changes are not noticeable in the age 8 to 70. Burger et al. [3], proposed an approach for automatic ear recognition. For Burger's method, each subject's ear is modeled as an adjacency graph built form Voronoi diagram of its curve segments. Victor et al. [4] and Chang et al. [5] used Eigen ear for identification. The results obtained were different in both cases. Chang's results show no difference in ear and face performance while Victor's results show that ear performance is worse than face. According to Chang views, the difference in result might be due to usage of different image quality. Another approach is proposed by Moreno et al. [6], this approach combines the results of neural classifier which use the information obtained from ear shape and wrinkles, and macro features extracted by compression network. Chen and Bhanu. [7] studied two steps iterative closest point algorithm on 30 people with their 3D ear images that were manually extracted. The results reveal 2 incorrect matching out of 60 images. In this paper, we present an effective ear features extraction and recognition based on multi-resolution Trace transform and modified Hausdorff distance combination.

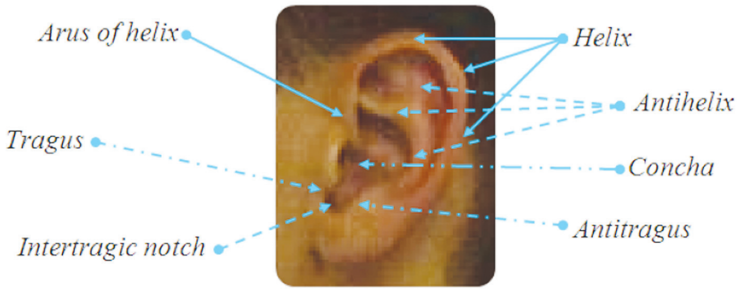

Figure 1. Ear's anatomy.

The rest of this paper follows. An introduction to the Trace transform, its properties and how it can be used to extract invariant features is given and the extraction of the identifier string from an ear image in Section 2. We describe a modified the Hausdorff distance in section 3. Finally, we present our experimental results in section 4, and Conclusion in section 5.

2. FEATURES EXTRACTION

2.1 Pre-processing

The ear part is manually cropped from the side face image and the portions of the ear which do not constitute the ear are colored white leaving only ear. And then, the colored ear image is converted to grayscale. The grayscale conversion is computed by:

$$GRAY_{x,y} = 0.299R_{x,y} + 0.587G_{x,y} + 0.114B_{x,y} \quad (1)$$

where R, G and B are color's value of each pixel in domain of red, green and blue. Figure 2.(b) shows the grayscale image which is obtained by cropping the ear part from the image in Figure 2.(a).

Figure 2. (a) A side face image acquired (b) Ear cropped grayscale image.

2.2 The Trace Transform

In this work, we use a trace transform technique for extracting features from clustered segments. The Trace transform [8, 9] method can produce feature values of an input image, invariant to translation, rotation and even reflection of an input image. Accordingly, it is suitable to extract feature values from various shapes of ear segments, even if deformed by translation, rotation, or reflection. The Trace transform projects all lines over an image and applies functional over these lines. A further functional, known as the diametrical functional, is applied to the Trace transform to obtain a one-dimension function known as the circus function. An ear image identifier is developed using the trace and diametrical functionals. A line is parameterized in a co-ordinate system C_l by (θ_1, d_1, t_1), as show in Figure 3.

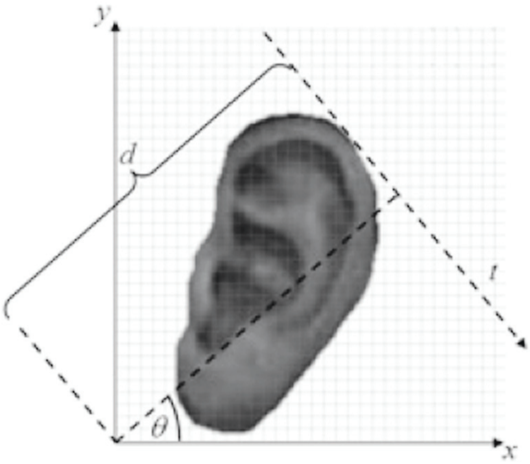

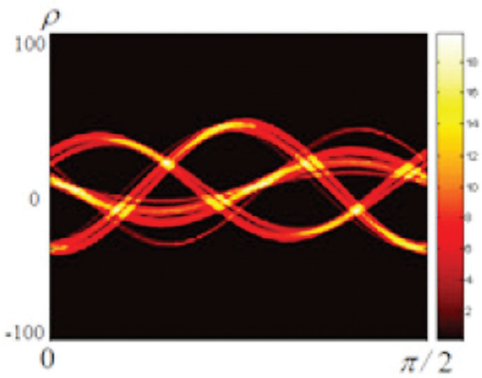

Figure 3. (a) The Trace transforms projects line over the ear image. The lines are parameterized by the angle θ and distance d. (b) The trace transform of ear image of (a) using functional *IF1*.

Where θ_1 the angle of the normal to the line is, d_1 is the distance between the origin and line and t_1 is the distance along the line. The values of the image function along a particular line are $F_1(\theta_1,d_1,t_1) = F(C_1;\theta_1, d_1,t_1)$. And then, the Trace transform T applies some functional over the image function that results in the diametrical function $d(C_1;\phi_1,\rho_1)= T(F(C_1;\phi_1, \rho_1, t_1))$. The diametrical functional D operates on the diametrical function to give the circus function

$$c(C_1;\phi_1)= D(T(C_1;\phi_1,\rho_1,t_1))). \qquad (2)$$

2.2.1 Invariant Functional

Shift invariance means that the value of the functional does not change if the function shifts. Examples are the integral, the median value, the maximal value of a function, etc. One might say that an invariant functional chooses an ordinate independently of the shift. A functional Ξ is called shift invariant if for any admissible function $\xi(x)$ is invariant if $\Xi(\xi(x+b)) = \Xi(\xi(x))$ for all $b \in \Re$ (Property I_1). The invariant functionals can have two further properties $\Xi(\xi(ax)) = \alpha(a)\Xi(\xi(x))$ for all $a > 0$ (Property i_1), and $\Xi(a\xi(x)) = \gamma(a)\ \Xi(\xi(x))$ for all $d > 0$ (Property i_2). It can be shown [8] that $\alpha(a) = a^{k_\Xi}$ and $\gamma(d) = d^{\lambda_\Xi}$, where the constants k_Ξ and λ_Ξ are called homogeneity constants of functional Ξ. Some invariant functionals and their properties are shown in Table 1.

Table 1. Invariant functionals and their properties.

No	Functional	k	λ	Properties
IF_1	$\int \xi(t)dt$	-1	1	I_1, i_1 and i_2
IF_2	$\left(\int \lvert \xi(t) \rvert^q \, dt\right)^r$	$-r$	qr	I_1, i_1 and i_2
IF_3	$\int \lvert \xi(t)' \rvert \, dt$	0	1	I_1, i_1 and i_2
IF_4	$\int (t - SF_1)^2 \xi(t)dt$	-3	1	I_1, i_1 and i_2
IF_5	$\sqrt{\frac{IF_4}{IF_1}}$	-2	0	I_1, i_1 and i_2
IF_6	$\max(\xi(t))$	0	1	I_1, i_1 and i_2
IF_7	$IF_6 - \min(\xi(t))$	0	1	I_1, i_1 and i_2

*** We have been used IF_1, IF_3 and IF_6 for this work.*

2.3 Multi-Resolution Trace T-ransform

Multi-resolution representations are popular technique for their powerful ability to describe signals at varying levels of detail from coarse gain to fine gain. Here a multi-resolution Trace transform is introduced that is quickly and efficiently generated from the original Trace transform. A Trace transform T with a specific functional provides one representation of an image. From this one abstraction a multi-resolution representation of the image can be generated which captures information at different scales. The Trace transform multi-resolution decomposition is performed by sub-sampling the original Trace transform of the image in either of its two dimensions, d or θ, or in both dimensions.

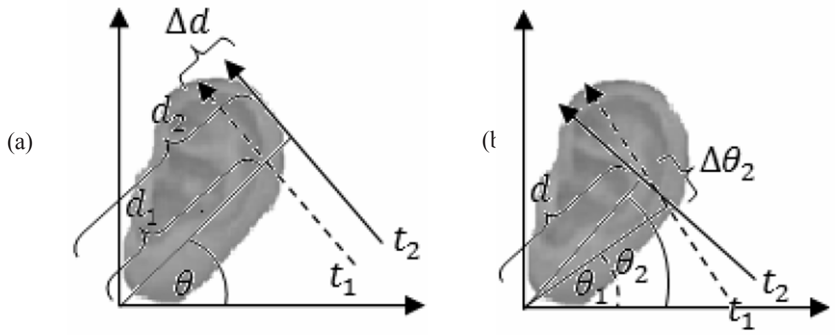

Figure 4. The multi-resolution Trace transform (a) with difference d (b) with difference θ.

This corresponds to projecting strips of width d over the image during the Trace transform, as shown in Figure 4(a). Sub-sampling also takes place by integrating over intervals in the parameter as shown in Figure 4(b).

2.4 The Identifier String Extr-action Algorithm

An image $f(x, y)$ can be viewed from two different co-ordinate systems C_1 and C_2. The coordinate system, C_2, is obtained from the C_1 by a rotation of angle $-\phi$, scaling the axis by parameter ν and by translating with the vector $(-S_0 \cos\varphi_0, -S_0 \sin \varphi_0)$. The image $f_2(\tilde{x}, \tilde{y})$ viewed from C_2, can be seen as the image $f_1(x, y)$ having undergone rotation by ϕ, scaling by $\nu-1$ and shifting by $(-S_0 \cos\varphi_0, -S_0 \sin \varphi_0)$. These linear transformations a line in f_1 will still be a line in f_2; the transformations are line preserving. The parameters of an image line in co-ordinate system C_1 in terms of the parameters of the line in C_2 are $\theta_1=\theta_2-\phi$, $d_1=\nu[d_2-S_0 \cos\varphi_0-\theta_2)$ and $t_1=\nu[t_2-S_0 \sin(\varphi_0-\theta_2)]$. From equation (1); it can be seen that the relationship of the circus function of an image in co-ordinate system C_2 to the image in coordinate system C_1 is given as

$$c(C_2;\phi_1)=D(T(F_1(\phi_1-\theta, \nu[\rho_1-S_0 \cos\varphi_0-\theta_0), \nu[t_1-S_0 \cos\varphi_0-\theta_1)]))) \quad (3)$$

The Trace functional T is chosen to obey I_1 and i_1

$$c(C_2;\phi_1)=D(\alpha_T(\nu)(F_1(\phi_1-\theta, \nu[\rho_1-S_0 \cos(\varphi_0-\theta_0)], t_1))) \quad (4)$$

Furthermore, the diametrical functional T can be chosen to obey I_1, i_1 and i_2 such that $c(C_2;\phi_2)=\gamma D(\alpha_T(\nu))D(T(F_1(\phi_1-\theta,\nu[\rho_1-S_0 \cos(\varphi_0-\phi_1)], t_1)))$, we obtain $c(C_2;\phi_2)= \gamma D(\alpha_T(\nu))\ \alpha_D(\nu)d(T(F_1(\phi_1-\theta,\rho_1 t_1)))$, and it can then be define as

$$c(C_2;\phi_1)= \kappa D(\alpha_T(\nu)) (F_1(\phi_1-\theta,\rho_1 t_1))), \quad (5)$$

where $\kappa = \gamma D(\alpha_T(\nu))\alpha_D(\nu)$. From equation (4) it can be seen that the one-dimension circus function in C_2 is a scaled and shifted version of the circus function in C_1. From equation (5) we taking the Fourier transform gives $F(\Phi) = \Im[\kappa D(T(F_l-\theta,\rho_1 t_1)))$ then exploiting the linearity identity and translation property of the Fourier Transform gives $F(\Phi) = \kappa \exp^{-j\theta\Phi} \Im[D(T(F_l(\phi_1-\theta,\rho_1,t_1)))]$. Taking the magnitude of $F(\Phi)$ gives

$$F(\Phi) = |\kappa \Im[D[T[F_l(\phi_1-\theta,\rho_1,t_1)))]|. \quad (6)$$

By the properties of the circus function and the magnitude of the Fourier transform an identifier can be extracted from an image. An algorithm to extract the binary identifier is given in Table 2. The identifier string [10] is very robust under similarity transform, which is scaling, rotation and translation (Table 2).

The multi-resolution Trace transform provides more identifiers. A one-dimensional decomposition over the distance (d) parameter is performed. The extraction process shown in table 2, steps 2 to 5, are used for each level of the multi-resolution Trace transform. Significant performance improvements are obtained by extracting multiple identifiers from each image. Firstly different identifiers are extracted by making different choices for the diametrical functionals in steps 1 and 2 of Algorithm-I (see in Table 2). In Table 2, the results are further improved by using different diametrical functionals to extract multiple component identifiers and con-catenating them to obtain a complete identifier as shown in Figure 5.

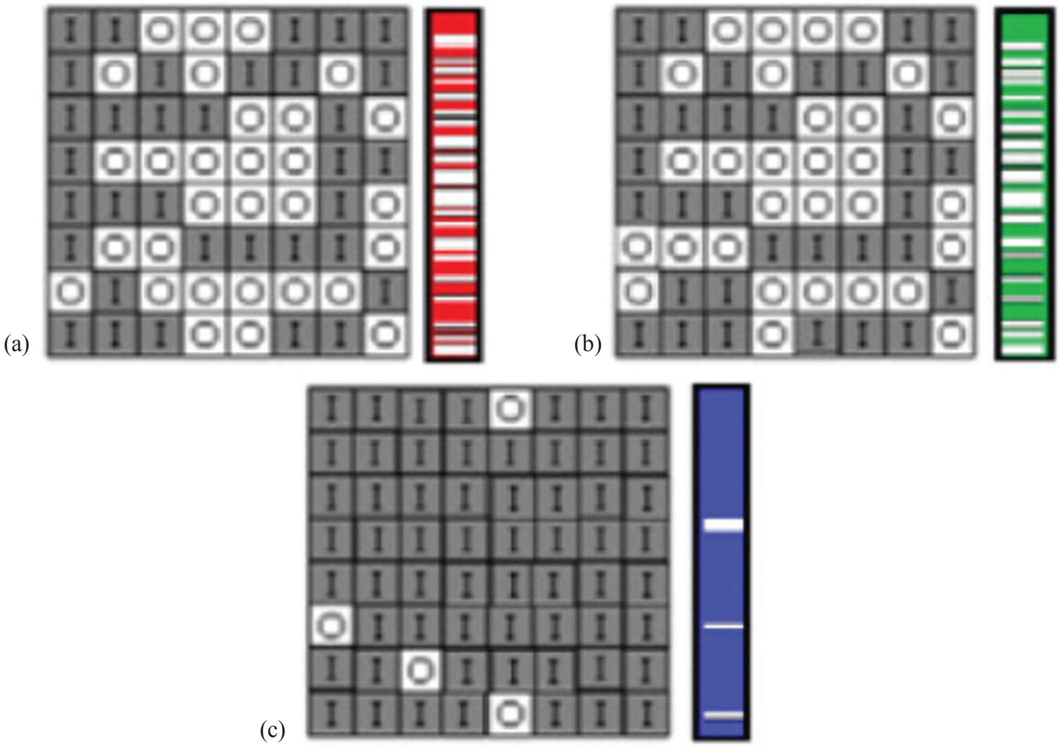

Figure 5. The identifier string of image (a) and its rotated version (b). The difference between the identifiers is show in (c).

Table 2. The binary identifier extraction algorithm.

Algorithm-I	
Step 1:	Take the Trace transform of the image using the functional $\int \xi(t)\,dt$ i.e., integrating over all lines in the image.
Step 2:	Find the first two circus functions by applying the following diametrical functionals to the columns of the two dimensions matrix resulting from step 1, $\int |\xi(t)'|\,dt$ where $'$ is the gradient max$\xi(t)$).
Step 3:	Get the magnitude of two circus functions by taking the Fourier transform.
Step 4:	Obtain the binary strings from each circus function that comes from taking the difference of neighboring coefficients $$i_\omega = \begin{cases} 0 & c(\omega) < 0 \\ 1 & otherwise \end{cases}, \qquad \text{(A.1)}$$ where $c(\omega)$ is defined by $c(\omega) = \lvert F(\omega) \rvert - \lvert F(\omega+1) \rvert$.
Step 5:	The first bit i1 corresponding to the different-combinations component is discarded and the identifier is made up of the subsequent N bits, $I=\{i_1, i_2, \ldots, i_n\}$.
Step 6:	For each diametrical functional perform steps (2) to step (5).
Step 7:	Concatenate each of the identifiers to obtain the complete identifier.

3. Similarity measure

3.1 Classical Hausdorff distance

Hausdorff distance [11] is a max-min distance that measures the extent to which two images are similar or different to one another. Therefore, Hausdorff distance can be used as a measure to determine the degree of resemblance between two objects. Given two point sets A and B, the Hausdorff distance between A and B is defined as

$$H(A,B) = \max(h(A,B),h(B,A)), \tag{7}$$

where

$$h(A,B)=\max_{a\in A} \min_{b\in B}\|a-b\|, \tag{8}$$

where $\|\bullet\|$ denotes some norm of points of A and B. This measure indicates the degree of similarity between two point sets. It can be calculated without an explicit pairing of points in their respective data sets. The conventional Hausdorff distance, however, is not robust to the presence of noise. A modified Hausdorff distance (MHD) using an average distance between the points of one set to the other set gives the best result. This measure is the most widely used in the task of object identification and defined as:

$$h(A,B) = \frac{1}{|A|}\sum_{a\in A}\min_{b\in B} \|a-b\|, \tag{9}$$

with $h(A,B)$ defined similarly. This modified Hausdorff distance is less sensitive to noise than the conventional one. It is possible, however, to end show the Hausdorff distance with even more attractive features as it is shown in the next section.

3.2 Sequentially Weighted Ha-usdorff Distance

The modified Hausdorff distance measure proposed in this paper is called Sequentially Weighted Hausdorff Distance (SWHD). Given two finite point sets $A=\{a_1,a_2,..,a_n\}$ and $B=\{b_1,b_2,..,b_n\}$, the sequentially weighted Hausdorff distance is defined as follows:

$$H_{sw}(A,B) = \max(h_{sw}(A,B), h_{sw}(B,A)). \tag{10}$$

The definition of the sequentially weighted directed Hausdorff distance $h_{sw}(A,B)$, as given:

$$h_{sw}(A,B) = \frac{1}{N_a} w(b) \min_{b\in B} \|a-b\|, \tag{11}$$

where $\|\bullet\|$ is an underlying norm on the points of A and B; Na is the number of points in set A; $w(x)$ is a weighted function, whose definition is:

$$w(x) = \begin{cases} N_R / N_S & \text{if} \quad N_R > 0 \\ 1 & \text{otherwise}, \end{cases} \tag{12}$$

where N_R is the number of remainder bit(s) in sub-sequentially and N_S is the number of total bit(s) in sub-sequentially (as show in Figure 6). However, the performance of h_{sw} depends on the completeness and incompleteness of the binary identifier extraction in section 2.3.

4. Experimental results

In this section, we describe a testing database we used and then present an ear recognition result under variant illumination, scaling, rotation. Our proposed method was implemented on the CMU PIE [12] database. Some sample testing images are show in Figure 7.

In the real-world applications, the image based recognition systems should be invariant to rotation, size variation, and illumination. In our proposed method, we use single image from the database for creating identifier string. The ear images for testing were generated by

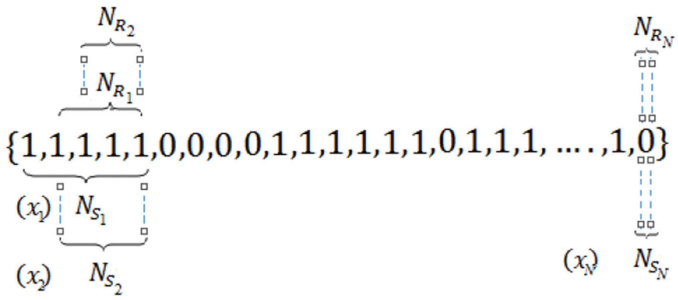

Figure 6. The Sequentially weighted Haus-dorff distance.

Figure 7. Some sample of CMU PIE data-base.

applying random scaling and rotation factors to the ear images, which were distributed within [1-50, 1+50] % and $[0, 360]^{o}$. Examples of test images are shown in Figure 8 and Table 3.

In summary, our proposed method is robust to rotation, size variation, and reflection. From the inspection of Table 3, it was found that our proposed method given the average accuracy rate is better than 97%. Such robustness comes from the use of Trace transform, Fourier transform, circus function, and matching measure in order of Section 2 and Section 3. Another advantage of our approach is that when new subjects are added to the system we do not need to retrain on the whole-ear database; in fact only images of the new subject are used to find the new optimal parameter of the algorithm. This may not be the case for the other traditional methods: when new subjects are added to the ear image database, these systems must be

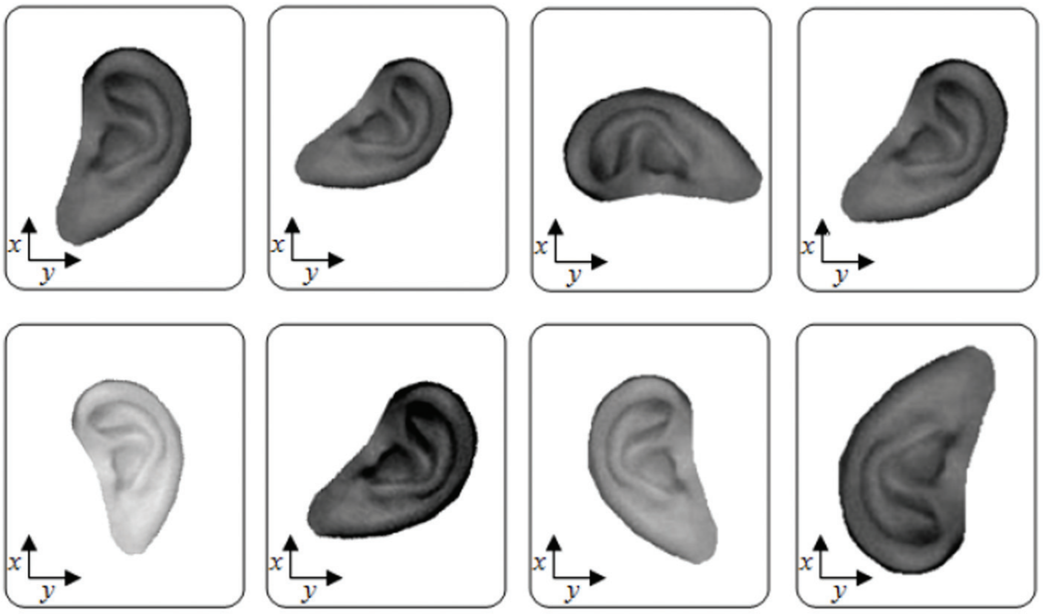

Figure 8. Examples of cropped ear images under rotation, size variation, blur, and reflection.

Table 3. Performance of our method.

Condition	Accuracy	Condition	Accuracy	Condition	Accuracy
Natural	≈ 100	Reflection	≈ 100	Rotation[±45°]	≈ 99
Side [±25%]	≈ 99	Bright [±5%]	≈ 98	Rotation[±90°]	≈ 99
Side [±50%]	≈ 95	Bright [±10%]	≈ 98	Rotation[±135°]	≈ 99
Side [±75%]	≈ 95	Bright [±15%]	≈ 96	Rotation[±180°]	≈ 99
Side [±100%]	≈ 94	Bright [±20%]	≈ 96	Rotation[±275°]	≈ 99

retrained over the whole-ear database, which is a barrier for real applications.

5. Conclusions

Our work proposes a highly robust method for ear based personal identification. Techniques introduced in this work are composed of two parts. The first one is the detection of image signatures by using the concepts of multi-resolution Trace transform, Fourier transform, and circus function. Then, in the second part, the notions of the modified Hausdorff distance and identifier string algorithm are employed to measure and to determine the similarity between the models and the tested images. Our method is evaluated with experiments on images from the CMU PIE database. The extensive experimental results show that the average of accuracy rate of ear recognition with variant scaling, rotation and image reflection is higher than 97 %.

Acknowledgement

This research was supported by Mahanakorn University of Technology. We would like to thank Carnegie Mellon University for providing the testing image databases.

REFERENCE

[1] Iannarelli A., *Ear Identification*, Forensic Identification Series, Paramount Publishing Company, 1989.

[2] Sforza C., Grandi G., Binelli M., Tommasi D.G., Rosati R. and Ferrario V. F., Age- and sex-related changes in the normal human ear, *Forensic Science International*, 2008; **187**: 110.e1-110.e7.

[3] Burger M. and Burger W., Ear Biometrics in Computer Vision, *Proc. of 15th Int. Con. on Pattern Recognition*, 2000; **12**: 2822.

[4] Victor B., Bowyer K. and Sarkar S., An Evaluation of Face and Ear Biometrics, *Proc. 16th Int. Conf. Pattern Recognition*, 2002; **1**: 429-432.

[5] Chang K., Bowyer K., and Barnabas V., Comparison and Combination of Ear and Face Images in Appearance-Based Biometrics, *IEEE Trans. Pattern Analysis and Machine Intelligence*, 2003; **25**: 1160-1165.

[6] Moreno B., Sanchez A. and Velez J.F., On the use of outer ear images for personal identification in security applications, *Proc. of IEEE Conf. On Security Technology,* 1999; **1**: 469-476.

[7] Chen H. and Bhanu B.,Contour Matching for 3D Ear Recognition, *Proc. 7th IEEE Workshop Application of Computer Vision*, 2005; **1**: 123-128.

[8] Petrou M. and Kadyrov A., Affine Invariant Features from the Trace Transform, *IEEE Trans. on Pattern Analysis and Machine Intelligence*, 2004; **26**: 30-44.

[9] Kadyrov A. and Petrou M., The Trace Transform and Its Applications, *IEEE Trans. Pattern Analysis and Machine Intelligence*, 2001; **23**: 811-828.

[10] Fooprateepsiri R. and Kurutach W., A Fast and Accurate Face Authentication Method Using Hamming-Trace Transform Combination, *IETE Technical Review*, 2010; **27**: 365-370.

[11] Huttenlocher P., Klanderman G. and Rucklidge W., Comparing Images using the Hausdorff Distance, *IEEE Trans. Pattern Analysis and Machine Intelligence*, 1993; **15**: 850-863.

[12] Sim T., Baker S. and Bsat M., The CMU Pose, Illumination, and Expression (PIE) Database, *Proc. the 2002 International Conference on Automatic Face and Gesture Recognition*, 2002; **1**: 46-51.